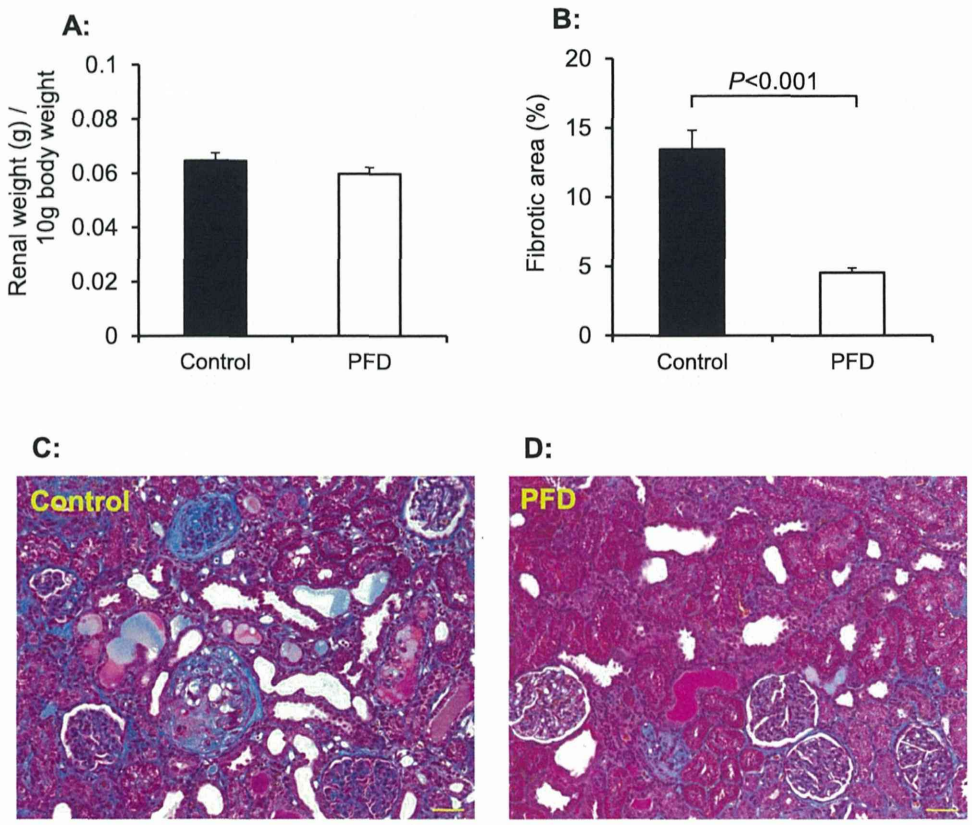

Fig. 2 Effects of PFD treatment on renal weight and fibrosis. (A) Relative renal weight in the Control (n = 10) and PFD (n = 10) groups at week 6; values represent renal organ weight per 10 g body weight. Renal weight was not significantly different between the Control and PFD groups. Representative images of the kidneys of the Control (C) and PFD (D) groups stained with Masson's trichrome exhibiting interstitial fibrosis and glomerular sclerosis (blue-colored area). PFD treatment markedly reduced the percentage of fibrotic areas (B).

pathways, including MAPK-family proteins (9). Also known as MAPKAPK3, 3pK is activated by three members of the MAPK family: extracellular signal-regulated kinase (ERK), p38MAPK, and Jun N-terminal kinase (JNK) (22). In the present study, renal 3pK protein levels were not significantly different between the Control and PFD groups (Fig. 3E). HIPK2 regulates renal fibrosis by activating the TGFβ pathway (18). In the present study, there was no significant difference between the Control and PFD groups with respect to HIPK2 protein expression (Fig. 3F).

From the results described above, we conclude that PFD exerts its renoprotective effect via down-regulation of the TGFβ and Smad2/3 signaling pathways.

Effects of PFD treatment on renal MMP/TIMP balance

MMP9 and its main inhibitor, TIMP1, play important roles in renal fibrosis (11, 21, 23). Nephritis-induced renal injury is more severe in MMP9-deficient mice than wild-type mice (21). Moreover, the significant rise of TIMP1 expression was attenuated by PFD in calcineurin inhibitor-induced nephrotoxicity (6). Therefore, the aim of the present study was to evaluate the effects of PFD treatment on renal MMP9/TIMP1 balance in hypertensive renal injury. Compared to the Control group, PFD treatment significantly increased renal MMP9 protein expression (Fig. 4A), whereas it significantly decreased that of renal TIMP1 (Fig. 4B).

Effects of PFD treatment on renal proliferation

FSP1, also called S100A4, is a specific fibroblast marker (37). In the present study, we did not observe significant suppression of fibroblast proliferation in renal interstitium after PFD treatment; we observed PFD treatment significantly attenuated the number of FSP1-positive cells in the fibrosis areas (Fig. 5).

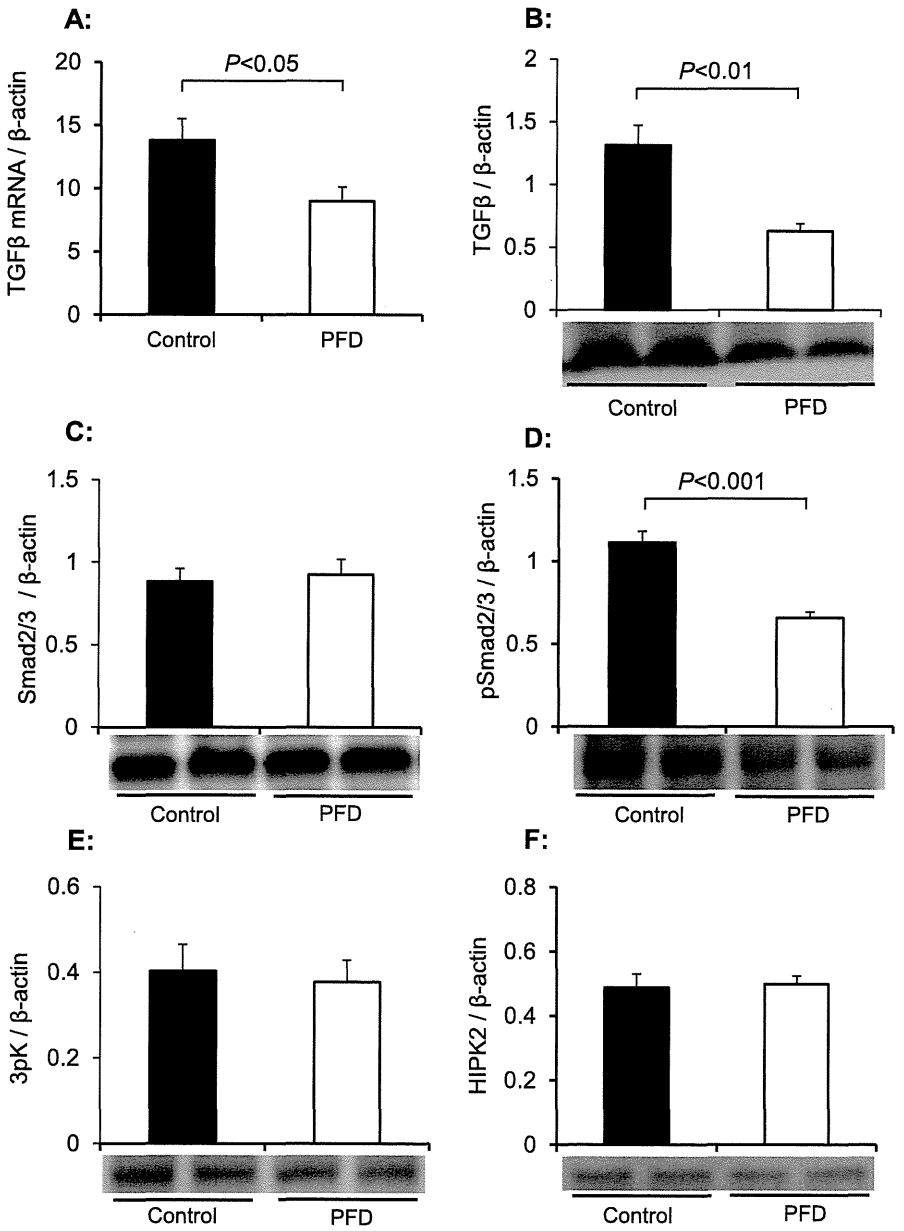

Fig. 3 Effects of PFD treatment on renal TGFβ, Smad2/3, pSmad2/3, 3pK, and HIPK2 expression. Expressions of TGFβ mRNA (A), TGFβ protein (B), Smad2/3 protein (C), pSmad2/3 protein (D), 3pK protein (E), and HIPK2 protein (F) in the kidneys of the Control and PFD groups. (n = 10 for Control and PFD groups)

Effects of PFD treatment on renal inflammatory reaction

To evaluate the renal inflammation caused by salt-induced hypertension, tissue sections of the kidneys were stained with CD68 (a macrophage marker) and CD3 (a T-cell marker). There were no significant differences between the Control and PFD groups with respect to macrophage (Fig. 6C) or T-cell infiltration (Fig. 6F).

PFD is reported to inhibit TNFα and IL1β expression (2, 12, 13, 20). However, we did not observe significant attenuation of renal TNFα protein expression (Fig. 6G) or plasma IL1β levels (Fig. 6H) after PFD treatment using Western blotting and ELISA, respectively.

Effects of PFD treatment on antioxidant activity

PFD was reported to have exhibited anti-oxidative stress effects in mesangial cells and in a cirrhosis model (27, 30). In the present study, a total antioxi-

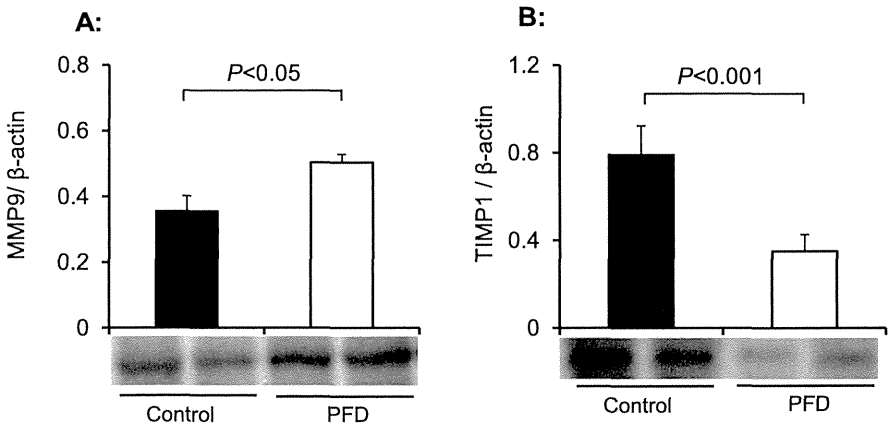

Fig. 4 Effects of PFD treatment on renal MMP/TIMP balance. PFD treatment significantly increased renal MMP9 protein expression (A). Renal TIMP1 protein levels in the PFD group were significantly lower than that in the Control group (B). (n = 10 for Control and PFD groups)

dant power kit was used to measure total serum antioxidant activity; we found that PFD treatment significantly increased the total antioxidant activity in serum (Fig. 7A; Control vs. PFD treatment, 10.17 ± 0.42 vs. 12.88 ± 0.76 nmol • mg protein^{-1}; $P < 0.05$). In addition, Western blotting revealed that PFD treatment significantly increased catalase protein expression in the kidneys (Fig. 7B).

DISCUSSION

PFD is a novel anti-fibrotic agent that inhibits the progression of renal fibrosis (1, 5–7, 24, 27, 34–36, 38). PFD has demonstrated anti-fibrotic, anti-inflammatory, and anti-oxidative stress effects in animal models and patients with renal diseases (6, 12–14, 27, 36). In the present study, we observed that PFD treatment decreased SBP, reduced proteinuria, and ameliorated renal fibrosis in a rat model of hypertensive renal injury.

TGFβ is a key protein in renal fibrosis (3, 4, 33), and PFD is an antagonist of TGFβ. PFD also decreases TGFβ expression in several animal nephropathy models (1, 5–7, 24, 27, 34–36, 38). In the present study, we also observed that PFD treatment decreased renal TGFβ mRNA and protein levels. TGFβ frequently modulates the transcription of key target genes via the Smad signaling pathway, which directly transduces TGFβ receptor activation to the nucleus (4, 9, 26, 31). In addition, Smad-independent signaling pathways via ERK, p38MAPK, and JNK provide alternative gene-activation mechanisms (9, 20).

In the present study, we observed that PFD treatment decreased Smad2/3 activity. In addition, renal 3pK protein levels were not significantly different between the Control and PFD groups. The uniqueness of 3pK is due to it being a novel convergence point of three MAPK pathways: ERK, p38MAPK, and JNK (22). From the results described above, we conclude that *1)* PFD treatment decreases renal TGFβ expression, which may mediate the downregulation of Smad2/3 activity; and *2)* the Smad-independent signaling pathways of ERK, p38MAPK, and JNK are not affected by PFD treatment upon renal injury and fibrosis. Recent reports also indicate that TGFβ and its downstream Smad pathway play important roles in renal diseases (4, 26, 31). In particular, PFD inhibits total Smad2/3 protein expression and TGFβ-induced Smad2 phosphorylation in murine mesangial cells (27). The balance between MMPs and TIMPs is also influenced by TGFβ in the kidneys (8, 10, 25). Furthermore, TGFβ stimulates fibroblast proliferation in the renal interstitium via a Smad-independent signaling pathway (39). From the results of the present and previous studies, we conclude that TGFβ is a potential central regulator of renal fibrosis. HIPK2 is reported to be a key regulator of renal fibrosis via the activation of the TGFβ-Smad3 pathway (18). However, PFD treatment did not affect HIPK2 protein expression in the kidneys in this study. This result suggests PFD treatment does not affect the TGFβ upstream signaling of HIPK2.

TIMP1 is the natural inhibitor of MMP9; both of these proteins play pivotal roles in kidney diseases. Therefore, disturbances in the balance of two systems lead to renal fibrosis (11, 21, 23). Nephritis-induced renal injury is more severe in MMP9-deficient mice than wild-type mice, which indicates that MMP9

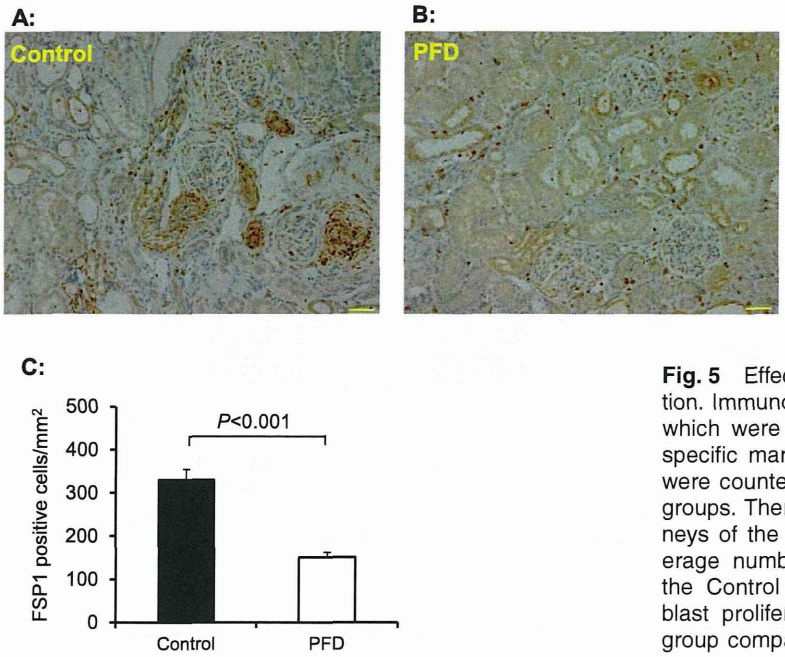

Fig. 5 Effects of PFD treatment on renal fibroblast proliferation. Immunohistochemical examination revealed fibroblasts, which were identified by positive staining for anti-FSP1 (a specific marker of fibroblasts) antibody. FSP1-positive cells were counted and compared between the Control and PFD groups. There were significantly more fibroblasts in the kidneys of the Control group (A) than the PFD group (B). Average numbers of immune cells per square millimeter in the Control (n = 10) and PFD (n = 10) groups (C). Fibroblast proliferation was significantly attenuated in the PFD group compared to the Control group.

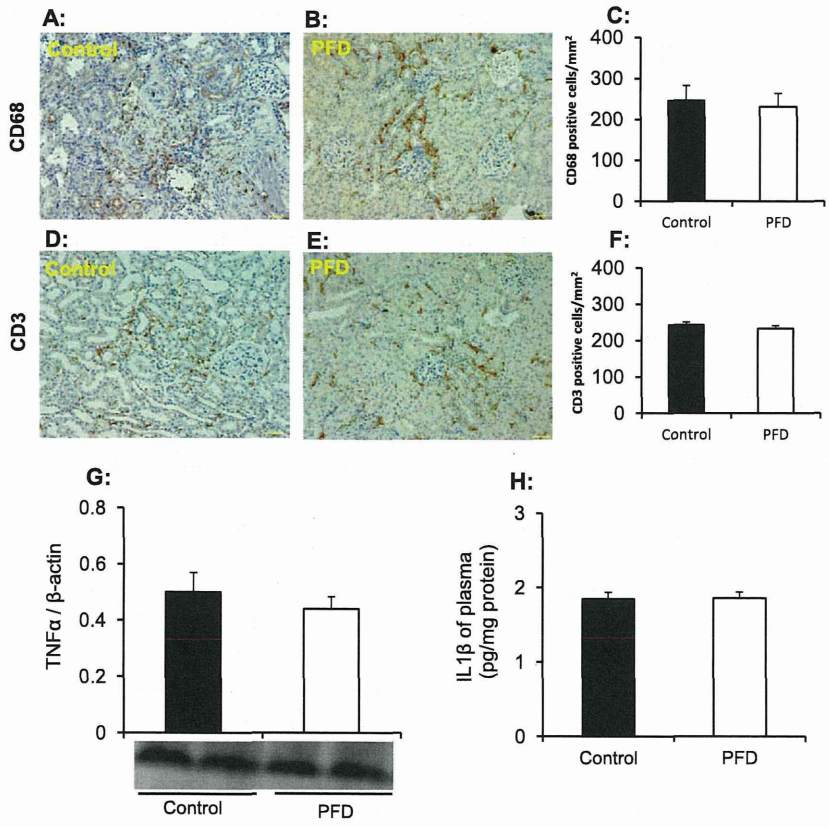

Fig. 6 Effects of PFD treatment on renal inflammatory reaction. Immunohistochemical examination revealed macrophages (A and B) and T cells (D and E), which were identified by positive staining for anti-CD68 and anti-CD3 antibodies, respectively. The numbers of cells positive for CD68 and CD3 were counted and compared between the Control and PFD groups. PFD treatment did not markedly attenuate macrophage (C) or T-cell (F) infiltration. Western blotting analysis also showed that PFD treatment did not significantly attenuate renal TNFα protein expression (G). ELISA revealed that PFD treatment did not affect the plasma level of IL1β (H). (n = 10 for Control and PFD treatment groups)

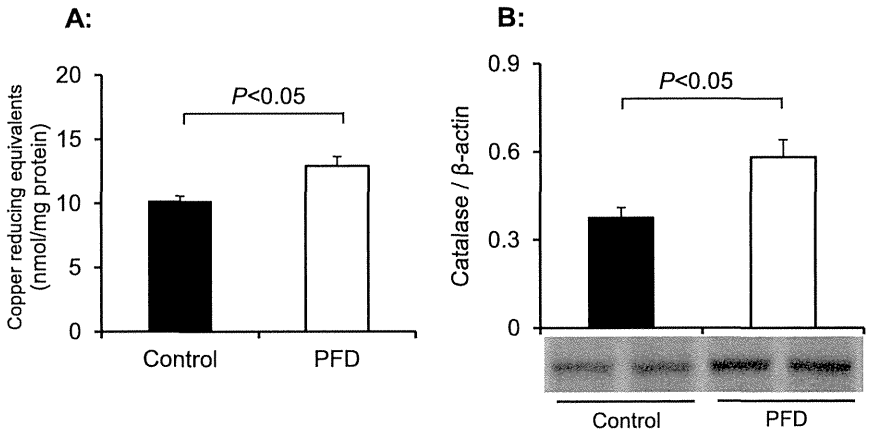

Fig. 7 Effects of PFD treatment on antioxidant activity. Total serum antioxidant activity was measured using the total antioxidant power kit. The activity level (expressed as copper-reducing equivalents) was significantly higher in the PFD group than the Control group after 6 weeks of high-salt diet intake (A). Western blotting showed that catalase expression was significantly higher in the PFD group than the Control group (B). (n = 10 for Control and PFD groups)

plays an important role in protecting renal function (21). Moreover, PFD affects MMP9/TIMP1 balance (6, 10, 20, 36). In the present study, PFD treatment increased MMP9 expression and decreased TIMP1 expression, suggesting that it may increase extracellular matrix degradation, leading to the attenuation of renal fibrosis.

PFD is also reported to attenuate renal fibroblast activation and proliferation *in vitro* (14). In the present study, PFD treatment significantly attenuated the number of FSP1-positive cells compared to the Control group. These results suggest that PFD treatment attenuates fibroblast proliferation; this may represent another possible mechanism of the anti-fibrotic effect of PFD.

From the results described above, we conclude that PFD exerts its anti-fibrotic effect via three mechanisms: *1)* downregulation of TGFβ-Smad2/3 signaling, *2)* improvement of MMP9/TIMP1 balance, and *3)* suppression of fibroblast proliferation (Fig. 8).

The association between renal inflammation and the development of renal fibrosis has been demonstrated in chronic kidney disease models (15, 16, 29). Moreover, PFD reduces the production of inflammatory mediators such as TNFα and IL1β (2, 12, 13, 20). Therefore, we also investigated the effects of PFD on inflammation in hypertension-induced renal injury. Unexpectedly, there were no significant differences between the Control and PFD groups with respect to macrophage or T-cell infiltration, namely TNFα protein expression or plasma levels of IL1β. From these results, we conjecture that PFD ameliorates the initial inflammation; however, if the injury continues toward end-stage renal disease, the anti-inflammatory effect of PFD is insufficient. Furthermore, the anti-fibrotic effect of PFD is the main mechanism that improves renal function.

Oxidative stress is also involved in progressive renal injury (28). Catalase deficiency promotes oxidant renal injury and fibrosis in mice (19). Moreover, PFD inhibited the production of reactive oxygen species in mesangial cells (27). We also observed that PFD treatment significantly increased renal catalase expression and total serum antioxidant activity. Therefore, we conclude that the anti-oxidative stress effect of PFD ameliorates renal injury and fibrosis.

Renal fibrosis can be induced via several mechanisms in different renal diseases but it ultimately produces identical fibrotic changes in the kidneys. In hypertension-induced renal injury, the therapeutic mechanisms of PFD are mediated by its anti-fibrotic and anti-oxidative stress pathways, not its anti-inflammatory pathway. PFD exerts its anti-fibrotic effect via three mechanisms: *1)* the downregulation of TGFβ-Smad2/3 signaling, *2)* improvement of MMP9/TIMP1 balance, and *3)* suppression of fibroblast proliferation (Fig. 8). TGFβ is a central regulator of renal fibrosis and is inhibited by PFD. Furthermore, PFD is a promising agent for the prevention of hypertensive renal injury. The clinical effectiveness of PFD has been evaluated in human diabetic nephropathy (32) and focal segmental glomerulosclerosis (7). Clarifying the renoprotective mechanisms of PFD will help us create new therapeutic strategies and could confer further benefits beyond the therapies currently used for the treat-

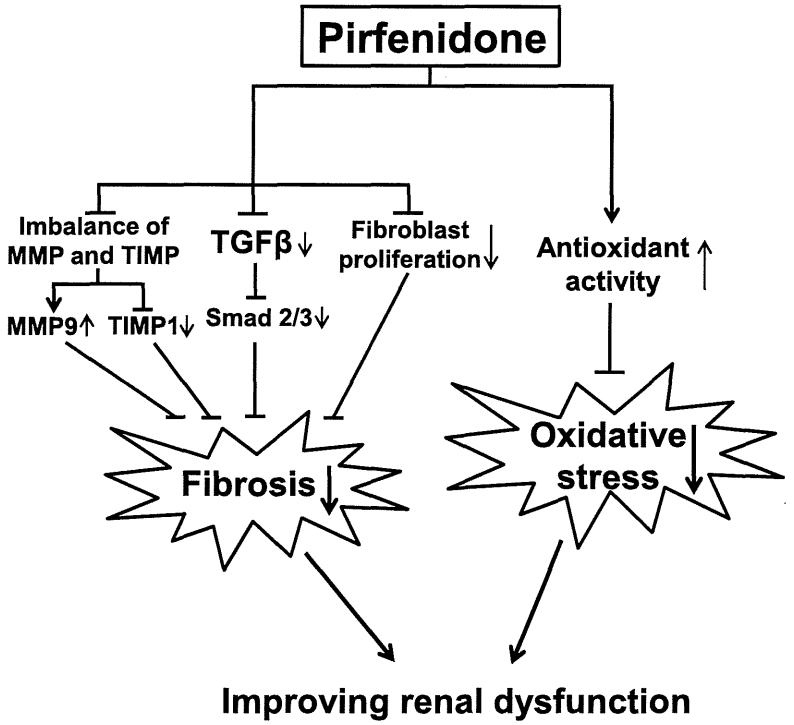

Fig. 8 The renoprotective mechanisms of PFD in hypertensive renal injury: through anti-fibrotic and anti-oxidative stress pathways. The therapeutic mechanisms of PFD on renal injury are mediated by its anti-fibrotic and anti-oxidative stress activities, not its anti-inflammatory activity. PFD exerts its anti-fibrotic effect via three pathways: (1) downregulation of TGFβ-Smad2/3 signaling, (2) improvement of MMP9/TIMP1 balance, and (3) suppression of fibroblast proliferation. TGFβ is a central regulator of renal fibrosis and is inhibited by PFD.

ment of chronic renal diseases.

Acknowledgements

We express our gratitude to Dr. Tomoko Ohya and Dr. Kyoko Shioya for their help. This work was supported in part by the Adaptable and Seamless Technology Transfer Program through Target-driven R&D, Japan (AS232Z02131G); the Program for the Promotion of Fundamental Studies in Health Science of the National Institute of Biomedical Innovation, Japan (Project ID: 10–24); the Grant-in-Aid for Scientific Research (C), Japan (23590705); the Health and Labour Sciences Research Grants, Japan (H24-food-004); and the Advanced Research for Medical Products Mining Programme of the National Institute of Biomedical Innovation (NIBIO), Japan.

REFERENCES

1. Al-Bayati MA, Xie Y, Mohr FC, Margolin SB and Giri SN (2002) Effect of pirfenidone against vanadate-induced kidney fibrosis in rats. *Biochem pharm* **64**, 517–525.
2. Arumugam TV, Shiels IA, Margolin SB, Taylor SM and Brown L (2002) Pirfenidone attenuates ischaemia-reperfusion injury in the rat small intestine. *Clin Exp Pharmacol physiol* **29**, 996–1000.
3. Border WA, Okuda S, Languino LR, Sporn MB and Ruoslahti E (1990) Suppression of experimental glomerulonephritis by antiserum against transforming growth factor beta 1. *Nature* **346**, 371–374.
4. Bottinger EP and Bitzer M (2002) TGF-beta signaling in renal disease. *J Am Soc Nephrol* **13**, 2600–2610.
5. Brook NR, Waller JR, Bicknell GR and Nicholson ML (2005) The experimental agent pirfenidone reduces pro-fibrotic gene expression in a model of tacrolimus-induced nephrotoxicity. *J Surg Res* **125**, 137–143.
6. Brook NR, Waller JR, Bicknell GR and Nicholson ML (2005) The novel antifibrotic agent pirfenidone attenuates the profibrotic environment generated by calcineurin inhibitors in the rat salt-depletion model. *Transplant Proc* **37**, 130–133.
7. Cho ME, Smith DC, Branton MH, Penzak SR and Kopp JB (2007) Pirfenidone slows renal function decline in patients with focal segmental glomerulosclerosis. *Clin J Am Soc Nephrol* **2**, 906–913.
8. Chromek M, Tullus K, Hertting O, Jaremko G, Khalil A, Li YH and Brauner A (2003) Matrix metalloproteinase-9 and tissue inhibitor of metalloproteinases-1 in acute pyelonephritis and renal scarring. *Pediatr Res* **53**, 698–705.
9. Derynck R and Zhang YE (2003) Smad-dependent and Smad-independent pathways in TGF-beta family signalling. *Nature* **425**, 577–584.
10. Di Sario A, Bendia E, Macarri G, Candelaresi C, Taffetani S, Marzioni M, Omenetti A, De Minicis S, Trozzi L and

Benedetti A (2004) The anti-fibrotic effect of pirfenidone in rat liver fibrosis is mediated by downregulation of procollagen alpha1(I), TIMP-1 and MMP-2. *Dig Liver Dis* **36**, 744–751.
11. Gonzalez-Avila G, Iturria C, Vadillo-Ortega F, Ovalle C and Montano M (1998) Changes in matrix metalloproteinases during the evolution of interstitial renal fibrosis in a rat experimental model. *Pathobiology* **66**, 196–204.
12. Grattendick KJ, Nakashima JM, Feng L, Giri SN and Margolin SB (2008) Effects of three anti-TNF-alpha drugs: etanercept, infliximab and pirfenidone on release of TNF-alpha in medium and TNF-alpha associated with the cell in vitro. *Int immunopharmacol* **8**, 679–687.
13. Hale ML, Margolin SB, Krakauer T, Roy CJ and Stiles BG (2002) Pirfenidone blocks the in vitro and in vivo effects of staphylococcal enterotoxin B. *Infect Immun* **70**, 2989–2994.
14. Hewitson TD, Kelynack KJ, Tait MG, Martic M, Jones CL, Margolin SB and Becker GJ (2001) Pirfenidone reduces in vitro rat renal fibroblast activation and mitogenesis. *J Nephrol* **14**, 453–460.
15. Ji X, Naito Y, Hirokawa G, Weng H, Hiura Y, Takahashi R and Iwai N (2012) P2X(7) receptor antagonism attenuates the hypertension and renal injury in Dahl salt-sensitive rats. *Hypertens Res* **35**, 173–179.
16. Ji X, Naito Y, Weng H, Endo K, Ma X and Iwai N (2012) P2X7 deficiency attenuates hypertension and renal injury in deoxycorticosterone acetate (DOCA)-salt hypertension. *Am J Physiol* **308**, F1207–2015.
17. Ji X, Takahashi R, Hiura Y, Hirokawa G, Fukushima Y and Iwai N (2009) Plasma miR-208 as a biomarker of myocardial injury. *Clin Chem* **55**, 1944–1949.
18. Jin Y, Ratnam K, Chuang PY, Fan Y, Zhong Y, Dai Y, Mazloom AR, Chen EY, D'Agati V, Xiong H, Ross MJ, Chen N, Ma'ayan A and He JC (2012) A systems approach identifies HIPK2 as a key regulator of kidney fibrosis. *Nat Med* **18**, 580–588.
19. Kobayashi M, Sugiyama H, Wang DH, Toda N, Maeshima Y, Yamasaki Y, Masuoka N, Yamada M, Kira S and Makino H (2005) Catalase deficiency renders remnant kidneys more susceptible to oxidant tissue injury and renal fibrosis in mice. *Kidney Int* **68**, 1018–1031.
20. Lee KW, Everett THt, Rahmutula D, Guerra JM, Wilson E, Ding C and Olgin JE (2006) Pirfenidone prevents the development of a vulnerable substrate for atrial fibrillation in a canine model of heart failure. *Circulation* **114**, 1703–1712.
21. Lelongt B, Bengatta S, Delauche M, Lund LR, Werb Z and Ronco PM (2001) Matrix metalloproteinase 9 protects mice from anti-glomerular basement membrane nephritis through its fibrinolytic activity. *J Exp Med* **193**, 793–802.
22. Ludwig S, Engel K, Hoffmeyer A, Sithanandam G, Neufeld B, Palm D, Gaestel M and Rapp UR (1996) 3pK, a novel mitogen-activated protein (MAP) kinase-activated protein kinase, is targeted by three MAP kinase pathways. *Mol Cell Biol* **16**, 6687–6697.
23. McMillan JI, Riordan JW, Couser WG, Pollock AS and Lovett DH (1996) Characterization of a glomerular epithelial cell metalloproteinase as matrix metalloproteinase-9 with enhanced expression in a model of membranous nephropathy. *J Clin Invest* **97**, 1094–1101.
24. Miric G, Dallemagne C, Endre Z, Margolin S, Taylor SM and Brown L (2001) Reversal of cardiac and renal fibrosis by pirfenidone and spironolactone in streptozotocin-diabetic rats. *Br J Pharmacol* **133**, 687–694.
25. Mo W, Brecklin C, Garber SL, Song RH, Pegoraro AA, Au J, Arruda JA, Dunea G and Singh AK (1999) Changes in collagenases and TGF-beta precede structural alterations in a model of chronic renal fibrosis. *Kidney Int* **56**, 145–153.
26. Piek E, Moustakas A, Kurisaki A, Heldin CH and ten Dijke P (1999) TGF-(beta) type I receptor/ALK-5 and Smad proteins mediate epithelial to mesenchymal transdifferentiation in NMuMG breast epithelial cells. *J Cell Sci* **112** (Pt 24), 4557–4568.
27. RamachandraRao SP, Zhu Y, Ravasi T, McGowan TA, Toh I, Dunn SR, Okada S, Shaw MA and Sharma K (2009) Pirfenidone is renoprotective in diabetic kidney disease. *J Am Soc Nephrol* **20**, 1765–1775.
28. Reddi AS and Bollineni JS (2001) Selenium-deficient diet induces renal oxidative stress and injury via TGF-beta1 in normal and diabetic rats. *Kidney Int* **59**, 1342–1353.
29. Rodriguez-Iturbe B, Pons H, Herrera-Acosta J and Johnson RJ (2001) Role of immunocompetent cells in nonimmune renal diseases. *Kidney Int* **59**, 1626–1640.
30. Salazar-Montes A, Ruiz-Corro L, Lopez-Reyes A, Castrejon-Gomez E and Armendariz-Borunda J (2008) Potent antioxidant role of pirfenidone in experimental cirrhosis. *Eur J Pharmacol* **595**, 69–77.
31. Schiffer M, Schiffer LE, Gupta A, Shaw AS, Roberts IS, Mundel P and Bottinger EP (2002) Inhibitory Smads and TGF-Beta signaling in glomerular cells. *J Am Soc Nephrol* **13**, 2657–2666.
32. Sharma K, Ix JH, Mathew AV, Cho M, Pflueger A, Dunn SR, Francos B, Sharma S, Falkner B, McGowan TA, Donohue M, Ramachandrarao S, Xu R, Fervenza FC and Kopp JB (2011) Pirfenidone for diabetic nephropathy. *J Am Soc Nephrol* **22**, 1144–1151.
33. Sharma K, Ziyadeh FN, Alzahabi B, McGowan TA, Kapoor S, Kurnik BR, Kurnik PB and Weisberg LS (1997) Increased renal production of transforming growth factor-beta1 in patients with type II diabetes. *Diabetes* **46**, 854–859.
34. Shihab FS, Bennett WM, Yi H and Andoh TF (2002) Pirfenidone treatment decreases transforming growth factor-beta1 and matrix proteins and ameliorates fibrosis in chronic cyclosporine nephrotoxicity. *Am J Transplant* **2**, 111–119.
35. Shimizu T, Fukagawa M, Kuroda T, Hata S, Iwasaki Y, Nemoto M, Shirai K, Yamauchi S, Margolin SB, Shimizu F and Kurokawa K (1997) Pirfenidone prevents collagen accumulation in the remnant kidney in rats with partial nephrectomy. *Kidney Int* **Suppl 63**, S239–243.
36. Shimizu T, Kuroda T, Hata S, Fukagawa M, Margolin SB and Kurokawa K (1998) Pirfenidone improves renal function and fibrosis in the post-obstructed kidney. *Kidney Int* **54**, 99–109.
37. Strutz F, Okada H, Lo CW, Danoff T, Carone RL, Tomaszewski JE and Neilson EG (1995) Identification and characterization of a fibroblast marker: FSP1. *J Cell Biol* **130**, 393–405.
38. Takakuta K, Fujimori A, Chikanishi T, Tanokura A, Iwatsuki Y, Yamamoto M, Nakajima H, Okada M and Itoh H (2009) Renoprotective properties of pirfenidone in subtotally nephrectomized rats. *Eur J Pharmacol* **629**, 118–124.
39. Wang S, Wilkes MC, Leof EB and Hirschberg R (2005) Imatinib mesylate blocks a non-Smad TGF-beta pathway and reduces renal fibrogenesis in vivo. *FASEB J* **19**, 1–11.

Lipids (2013) 48:803–815
DOI 10.1007/s11745-013-3805-3

ORIGINAL ARTICLE

Three Dissimilar High Fat Diets Differentially Regulate Lipid and Glucose Metabolism in Obesity-Resistant Slc:Wistar/ST Rats

Yoko Hashimoto · Kazuyo Yamada · Hiromi Tsushima · Daisuke Miyazawa · Mayumi Mori · Koji Nishio · Takeshi Ohkubo · Hidehiko Hibino · Naoki Ohara · Harumi Okuyama

Received: 25 December 2012 / Accepted: 15 May 2013 / Published online: 27 June 2013

Abstract Epidemiologic and ecologic studies suggest that dietary fat plays an important role in the development of obesity. Certain Wistar rat strains do not become obese when fed high-fat diets unlike others. In a preliminary study, we confirmed that Slc:Wistar/ST rats did not become obese when fed high-fat diets. The mechanisms governing the response of hepatic lipid-metabolizing enzymes to large quantities of dietary lipids consumed by obesity-resistant animals are unknown. The aim of the present study is to examine how obesity-resistant animals metabolize various types of high-fat diets and why they do not become obese. For this purpose, male Slc:Wistar/ST rats were fed a control low-fat diet (LS) or a high-fat diet containing fish oil (HF), soybean oil (HS), or lard (HL) for 4 weeks. We observed their phenotypes and determined lipid profiles in plasma and liver as well as mRNA expression levels in liver of genes related to lipid and glucose metabolism using DNA microarray and quantitative reverse transcriptase polymerase chain analyses. The body weights of all dietary groups were similar due to isocaloric intakes, whereas the weight of white adipose tissues in the LS group was significantly lower. The HF diet lowered plasma lipid levels by accelerated lipolysis in the peroxisomes and suppressed levels of very-low-density lipoprotein (VLDL) secretion. The HS diet promoted hepatic lipid accumulation by suppressed lipolysis in the peroxisomes and normal levels of VLDL secretion. The lipid profiles of rats fed the LS or HL diet were similar. The HL diet accelerated lipid and glucose metabolism.

Keywords High-fat diet · Soybean oil · Fish oil · Lard · Plasma lipids · Hepatic lipids · Gene expression

Abbreviations

DHA	Docosahexaenoic acid (22:6n-3)
EPA	Eicosapentaenoic acid (20:5n-3)
LNA	Linoleic acid (18:2n-6)
MUFA	Monounsaturated fatty acid(s)
NEFA	Non-esterified fatty acid
PUFA	Polyunsaturated fatty acid(s)
RT-PCR	Reverse transcriptase-polymerase chain reaction
SDS-PAGE	Sodium dodecyl sulfate-polyacrylamide gel electrophoresis
SFA	Saturated fatty acid(s)
TAG	Triacylglycerol(s)

Y. Hashimoto (✉)
Department of Biochemistry, School of Dentistry, Aichi-Gakuin University, 1-100 Kusumoto-cho, Chikusa-ku, Nagoya 464-8650, Japan
e-mail: yokuteku@dpc.agu.ac.jp

K. Yamada · H. Tsushima · D. Miyazawa · N. Ohara · H. Okuyama
Open Research Center, Kinjo Gakuin University College of Pharmacy, Omori, Moriyama-ku, Nagoya, Japan

M. Mori
Department of Pharmacology, Nagoya City University Graduate School of Medical Science, Kawasumi, Mizuho-ku, Nagoya, Japan

K. Nishio
Department of Anatomy and Neuroscience, Nagyoya University Graduate School of Medicine, 65 Tsurumai-cho, Showa-ku, Nagoya, Japan

T. Ohkubo · H. Hibino
NOF Corporation, Chidori-cho, Kawasaki-ku, Kanagawa, Japan

Introduction

The incidence of obesity, metabolic syndrome, and diabetes mellitus is increasing globally to epidemic levels [1]. To address this issue, a more detailed understanding of these disease processes is urgently required [1]. Excessive intake of lipids is considered an etiological factor for the development of obesity [2]. In contrast, dietary fats and oils are important sources of energy, essential fatty acids, and fat-soluble vitamins. Moreover, they influence the profiles of lipids in plasma and liver [3–7]. Increased plasma cholesterol levels have been proposed to accelerate the development of atherosclerosis and increase the risk of coronary heart disease (CHD) [8], although other evidence indicates the opposite [9]. Dietary vegetable oils enriched in n-6 polyunsaturated fatty acid (n-6 PUFA) were proposed to induce lower serum cholesterol levels [10, 11]. However, this effect is transient, and excessive intake of n-6 PUFA increased the incidence of CHD [9]. In contrast, a diet containing fish oils rich in n-3 PUFA, such as eicosapentaenoic acid (EPA, 20:5n-3) and docosahexaenoic acid (DHA, 22:6n-3), delays the development of atherosclerosis [12] and reduces the incidence of CHD [3, 13–15]. The atherosclerosis-related diseases involved in inflammation and are caused by overexpression of cyclooxygenase (COX, EC 1.14.99.1) [16]. Different types of dietary fatty acids have been implicated in atherosclerosis and CHD, possibly through different mechanisms. To prevent and overcome these diseases, it is important to understand the different effects of various types of dietary high fats on lipid and glucose metabolism.

High-fat diets induce obesity and metabolic disorders in rodents that resemble the human metabolic syndrome [17]. Wistar rats are susceptible to obesity when fed high-fat diets [17]. Buettner et al. [7] reported that high-fat diets containing 42 energy % (en%) lard, olive oil, or coconut fat induced obesity in Wistar rats, although it was emphasized in a review [17] that the phenotype induced by high-fat diets varied distinctly among different studies. In fact, Piche et al. [18] did not observe a significant difference in the food intake and body weight of Wistar rats fed a diet supplemented with 10 % (approximately 22 en%) lard, corn oil, soybean oil, canola oil, or cod liver oil. Rand et al. [19] also fed Wistar rats with diets supplemented with 50 en% of sunflower oil or palm oil and found no significant difference in the body weights compared with feeding a low-fat laboratory chow. Substrains of Wistar rats kept in different laboratories may exhibit different obesity-related phenotypes. In a preliminary experiment, we confirmed that Slc:Wistar/ST rats did not become obese under our conditions when fed high-fat diets. Therefore, this strain was used in the present study as a model resistant to obesity.

Genetically obese animals have been the focus of research on obesity and metabolic syndrome [17], and animals that do not develop obesity have served mainly as controls. Little is known about how obesity-resistant animals metabolize various types of high-fat diets. A detailed comparison of the differential effects of various high-fat diets on lipid parameters influenced by lipid and glucose metabolism has yet to be investigated in obesity-resistant animals. Therefore, we examined the effects of various high-fat diets on plasma and hepatic lipid parameters and lipid metabolism using Slc:Wistar/ST rats that do not develop obesity. For this purpose, we maintained male rats on 3 different high-fat diets (HF, fish oil; HS, soybean oil; HL, lard) for 4 weeks and determined their body and tissue weights, total food consumption, oil composition, and energy metabolism, and lipid profiles of plasma and liver. The data were compared with those of rats fed a low-fat diet (LS, soybean oil supplemented), and those of obesity-susceptible animals.

To understand the molecular basis of the effects of these high-fat diets (HF, HS and HL), we took advantage of microarray technology, which is a useful tool for high-throughput quantitative analysis of gene expression [20]. This method has evolved rapidly during the past decade with dramatic improvements in probe selection, sensitivity, image acquisition, and data analysis. The liver plays central roles in lipid, glucose, and cholesterol metabolism. The close connection between lipid and glucose metabolism maintains energy homeostasis [21]. Therefore, the expression levels of 326 genes associated with lipid and glucose metabolism were analyzed using DNA microarrays. Moreover, the mRNA expression levels of 19 genes involved in inflammatory responses as well as lipid metabolism were examined using quantitative reverse transcriptase polymerase chain reaction (qRT-PCR) analysis. To complement gene transcription analysis, we determined the expression levels and identities of hepatic proteins using sodium dodecyl sulfate-polyacrylamide gel electrophoresis (SDS-PAGE) and matrix-assisted laser desorption/ionization-time of flight (MALDI-TOF) mass spectrometry (MS). The mechanisms by which various fatty acids differentially alter the lipid profiles in the liver and plasma of male Wistar rats were revealed based on the data obtained from these techniques.

Slc:Wistar/ST rats did not become obese when fed high-fat diets, because their caloric intakes were similar and independent of the type and amount of dietary fatty acids. However, the weights of visceral white adipose tissues (WAT) were significantly greater in the high-fat dietary groups than in the low-fat dietary group. The HF diet lowered plasma lipid levels by stimulated peroxisomal β-oxidation and suppressed very-low-density lipoprotein (VLDL) secretion. The HS diet induced hepatic lipid accumulation via suppression of peroxisomal β-oxidation

and normal levels of VLDL secretion. The hepatic and plasma lipid profiles of rats fed the HL and LS diets were similar. The HL diet did not induce hepatic lipid accumulation. Lipid and glucose metabolism were accelerated in rats fed the HL diet. This study, to our knowledge, is the first to show the differential effects of 3 high-fat diets on lipid and glucose metabolism in Slc:Wistar/ST rats.

Materials and Methods

Animals and Diets

Male Slc:Wistar/ST rats (specific-pathogen-free) at 4 weeks-of-age were purchased from Japan SLC, Inc., Hamamatsu, Japan and were housed two per cage with a 12-h light–dark cycle at 23 °C under controlled environmental conditions. The experiments were carried out according to the Guidelines for Animal Care and Use, and the protocols for the experiments were approved by the Institutional Animal Care and Use Committee of Kinjo Gakuin University College of Pharmacy. We prepared high-fat (20 % w/w) diets by mixing fish oil, soybean oil, or lard with normal (conventional) low-fat powdered diet (F-1 fish meal-free containing 4.4 % w/w lipid by weight of which 1.7 % w/w was soybean oil) (Funabashi Farm Co., Ltd.; Chiba, Japan). The final oil content of high-fat diets was 23.5 % (w/w). Total energy content and fat energy were 468.0 kcal/100 g and 45.2 en% and 360.0 kcal/100 g and 11.0 en%, respectively, for the high-fat diets and normal low-fat diet (LS). After feeding the LS diet for 1 week, rats were divided randomly into 4 groups, 6 animals/group, and maintained for 4 weeks with free access to the LS, HF, HS, HL diets and water. The powdered diet was provided in a container with a dome-shaped cover (Roden Café: Oriental Yeast Co., Ltd.; Tokyo, Japan) to prevent the diet from dropping out of the container and to prevent contamination with wood chips entering into the container. The remaining diet was weighed, discarded, and replenished 3 times a week. Body weight was measured weekly.

Determination of Fatty Acid Compositions of Diets

The lipids in the experimental diets were extracted with chloroform/methanol according to the method of Bligh and Dyer [22], and the fatty acid compositions were determined by gas chromatography as described elsewhere [23].

Determination of Lipid and Protein Profiles in Plasma and Liver

Rats were fasted overnight and anesthetized with sevoflurane, and then euthanized by cardiac puncture. Blood was collected in a tube containing EDTA. The plasma was separated by centrifugation at 3,000 rpm for 15 min at 4 °C, and stored at −80 °C. The livers and hearts were weighed, frozen in dry ice-acetone (−78 °C), and then stored at −80 °C. The epididymal white adipose tissue (WAT), perirenal WAT, and brown adipose tissue (BAT) were isolated and weighed. The total visceral WAT is defined as the weight of epididymal fat tissues and perirenal fat tissues. Liver samples for mRNA analysis were transferred into the RNAlater® solution (Ambion Cat # AM7020) to prevent RNA degradation during storage. Glucose, total cholesterol (t-Cho), triacylglycerol (TAG), HDL-cholesterol (HDL-C), non-esterified fatty acid (NEFA), and total protein (TP) present in plasma were measured using a clinical auto-analyzer (TMS-1024: Tokyo Boeki Medical System Ltd.; Tokyo, Japan). Approximately 100 mg of the liver was homogenized in phosphate buffered saline (PBS), and the homogenate was then divided into two portions to measure protein and lipid concentrations. The lipids were extracted from the homogenate 3 times with chloroform/methanol according to the method of Bligh and Dyer [22] as mentioned above and were extracted from the organic phase dried under N_2 gas, and solubilized with isopropanol containing 10 % Triton X-100. The levels of hepatic t-Cho, NEFA, phospholipid (PL), and TAG were measured using Wako assay kits as follows: L-type Wako CHO M, NEFA C-test Wako, L-type Wako phospholipid, and L-type Wako TG M. All assay kits and a Multi-Calibrator Lipid standard were purchased from Wako Pure Chemical Industries Ltd., Osaka, Japan. The protein concentration of the liver was determined by the method of Hartree [24] using bovine serum albumin (Sigma-Aldrich Co., St. Louis, MO) as a standard.

DNA Microarray Analysis

RNA was extracted from liver samples using an RNeasy Protect Mini Kit (Qiagen, Valencia, CA) combined with DNase I according to the manufacturer's instructions. Total RNA was quantified by absorbance at 260 nm. Two micrograms of RNA from 6 samples of each group were pooled and the expression levels of 326 genes (http://www.kurabo.co.jp) associated with lipid and glucose metabolism were analyzed using a GeneSQUARE (Kurabo Industrial Ltd.; Osaka, Japan) multi-sample DNA microarray system. Sample processing and data acquisition were carried out by Kurabo Industrial Ltd. Gene expression levels of the HF, HS, or HL groups were normalized to those of the LS group and the values of experimental groups were expressed as fold changes, which are ratios to those of the LS group. Significant differences were judged from fold changes of ≥ 2.0 or ≤ 0.5.